Metals **2015**, *5*, 656-668; doi:10.3390/met5020656

OPEN ACCESS

metals

ISSN 2075-4701

www.mdpi.com/journal/metals/

Article

Development of Nanocrystalline 304L Stainless Steel by Large Strain Cold Working

Marina Odnobokova, Andrey Belyakov * and Rustam Kaibyshev

Belgorod State University, Pobeda 85, Belgorod 308015, Russia;
E-Mails: odnobokova@bsu.edu.ru (M.O.); rustam_kaibyshev@bsu.edu.ru (R.K.)

* Author to whom correspondence should be addressed; E-Mail: belyakov@bsu.edu.ru;
Tel.: +7-4722-585457; Fax: +7-4722-585417.

Academic Editor: Heinz Werner Höppel

Received: 29 March 2015 / Accepted: 14 April 2015 / Published: 22 April 2015

Abstract: The microstructural changes leading to nanocrystalline structure development and the respective tensile properties were studied in a 304L stainless steel subjected to large strain cold rolling at ambient temperature. The cold rolling was accompanied by the development of deformation twinning and martensitic transformation. The latter readily occurred at deformation microshear bands, leading the martensite fraction to approach 0.75 at a total strain of 3. The deformation twinning followed by microshear banding and martensitic transformation promoted the development of nanocrystalline structure consisting of a uniform mixture of austenite and martensite grains with their transverse sizes of 120–150 nm. The developed nanocrystallites were characterized by high dislocation density in their interiors of about 3×10^{15} m^{-2} and 2×10^{15} m^{-2} in austenite and martensite, respectively. The development of nanocrystalline structures with high internal stresses led to significant strengthening. The yield strength increased from 220 MPa in the original hot forged state to 1600 MPa after cold rolling to a strain of 3.

Keywords: austenitic stainless steel; severe plastic deformation; deformation twinning; strain-induced martensite; grain refinement; nanocrystalline structure; strengthening

---

1. Introduction

The large strain deformations are considered as promising methods for development of advanced structural steels and alloys with enhanced mechanical properties [1,2]. The significant improvement of mechanical properties of metallic materials subjected to severe plastic deformations is commonly attributed to the strain-induced ultrafine-grained or, even, nanocrystalline structures [3–5]. The ultrafine-grained materials have been shown to possess a unique combination of high strength and surprisingly large ductility [6]. The efficiency of cold working for processing the high-strength ultrafine-grained/nanocrystalline products depends remarkably on the kinetics of grain refinement during plastic deformation. Austenitic stainless steels are typical representative of metallic materials exhibiting rapid grain refinement upon cold working [7–10]. The grain refinement in these steels is promoted by an intensive grain subdivision, which is associated with deformation twinning followed by strain-induced martensitic transformation [9–13]. Therefore, the austenitic stainless steels can be easily produced in high-strength ultrafine-grained/nanocrystalline state by conventional cold working technique like plate rolling [10]. In spite of a number of research works dealing with nanocrystalline stainless steels processed by large strain cold working, however, the mechanisms of microstructure evolution, *i.e.*, a role of deformation twinning and strain-induced martensite, and their contribution to strengthening are still unclear.

The strengthening of metallic materials processed by large strain deformation is generally discussed in terms of either grain boundary strengthening [14] or dislocation strengthening [15,16]. The former is commonly evaluated as $\sigma_{GB} = K_\varepsilon D^{-0.5}$, where D is the grain size and K_ε is a constant; and the latter is related to a square root of dislocation density as $\sigma_{DISL} = \alpha G b \rho^{0.5}$, where α, G, and b are a constant, the shear modulus, and the Burgers vector, respectively. Assuming that the grain boundary strengthening and the dislocation strengthening contribute independently to overall strength, a modified Hall-Petch-type relationship has been recently introduced to relate the yield strength of ultrafine-grained/nanocrystalline materials processed by severe plastic deformation to their microstructural parameters, *i.e.*, the grain size and dislocation density, in the following form [17–19]:

$$\sigma_{0.2} = \sigma_0 + K_\varepsilon D^{-0.5} + \alpha G b \rho^{0.5} \quad (1)$$

Here, σ_0 is the strength of dislocation-free single crystal. Recent studies on severely deformed quasi-single phase ultrafine-grained/nanocrystalline materials have shown that the contribution from dislocation strengthening exceeds remarkably that from grain boundaries [20,21]. However, the strengthening mechanisms for ultrafine-grained/nanocrystalline materials such as metastable austenitic stainless steels, which experience martensitic phase transformation during cold working, have not been studied.

The aim of this study is to clarify the microstructural operating mechanisms, which are mainly responsible to the development of nanocrystalline structure in a typical chromium-nickel stainless steel during large strain cold rolling, and to investigate the strengthening mechanisms of the cold rolled steel, namely, the relationship between the microstructural parameters and strength contributions.

2. Experimental Section

A 304L-type austenitic steel (Fe-0.05%C-18.2%Cr-8.8%Ni-1.65%Mn-0.43%Si-0.05%P-0.04%S, all in wt%) with an initial grain size of 21 μm was hot forged and annealed at 1100 °C followed by air cooling. The plate rolling was carried out on samples with an initial cross section of 30 × 30 mm^2 at room temperature to various total true strains up to 3. In order to clarify the conventional Hall-Petch relationship for the present steel, several rolled samples were annealed to various recrystallized grain sizes at temperatures of 900–1150 °C. The strain hardening was studied by Vickers hardness tests with a load of 3 N. The microstructural characterization was performed using a JEM-2100 transmission electron microscope (TEM, JEOL Ltd., Tokyo, Japan) and a Nova Nanosem 450 scanning electron microscope equipped with an electron back-scatter diffraction (EBSD) analyzer (FEI, Hillsboro, OR, USA) on the sample sections normal to the transverse direction. The volume fractions of the ferrite were averaged through X-ray analysis, magnetic induction method and EBSD technique. The transverse grain size was measured on EBSD micrographs by a linear intercept method along the normal direction. The dislocation density was estimated by counting individual dislocations revealed by TEM in the grain/subgrain interiors. The tensile tests were carried out at room temperature by using specimens with a gage length of 6 mm and width of 3 mm. The equilibrium phase content was calculated with ThermoCalc software using TCFE6 database (ThermoCalc Software, Stockholm, Sweden).

3. Results and Discussion

3.1. Strain Hardening and Phase Transformation

The effects of cold rolling on the hardness and strain-induced martensite fraction are shown in Figure 1. The hardness drastically increases from about 1360 MPa to 4000 MPa during cold rolling to a total strain of 0.5. Then, the rate of strain hardening gradually slows down leading to a progressive increase in the hardness to above 5200 MPa as the total strain increases to 3. In contrast to strain hardening, the fraction of strain-induced martensite almost linearly increases with strain in the strain range of $0 < \varepsilon < 2$. Upon further rolling, the kinetics of the phase transformation becomes sluggish leading the strain-induced martensite fraction to approach 0.75, which is close to its saturation value of about 0.85 as predicted by ThermoCalc. It should be noted in Figure 1 that there is no direct correlation between the strain hardening and the martensite transformation. In other words, the change in hardening rate during the rolling does not provide similar change in the martensite fraction. Remarkable increase in the martensite fraction from 0.2 to 0.65 occurs in the strain range from 0.5 to 2, while the hardness increase does not exceed 20%.

3.2. Microstructure Evolution

Typical deformation microstructures that developed during cold rolling to different total strains are shown in Figure 2. The deformation microstructures combined with the inverse pole figures for the normal direction (vertical in Figure 2) are shown in left-hand figures, whereas the right-hand figures represent the austenite/martensite phase distribution. An early deformation is accompanied by the frequent development of deformation twinning, which is typical feature of austenitic steels with low

stacking fault energy [9,10,13,20], followed by the martensitic transformation. Further deformation results in a flattening of the original grains and the development of microshear bands. The latter ones serve as preferential nucleation sites for the strain-induced martensite [11,22,23], resulting in significant increase in the martensite fraction at intermediate strains of around 1 as mentioned before in Figure 1. The grain flattening and the microshearing result in the wavy microstructure at large rolling strains. This microstructure is mainly composed by the strain-induced martensite, since its fraction comprises 0.75 at a large strain of 3. Therefore, the largely strained microstructure consists of highly elongated wavy martensite grains interleaved with chains of fine austenite grains.

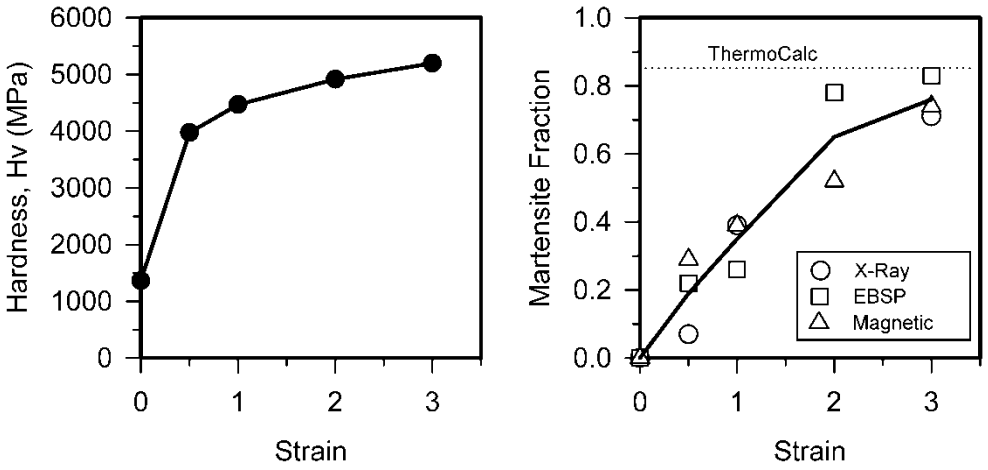

Figure 1. The effect of cold rolling strain on the hardness and strain-induced martensite fraction in a 304L stainless steel.

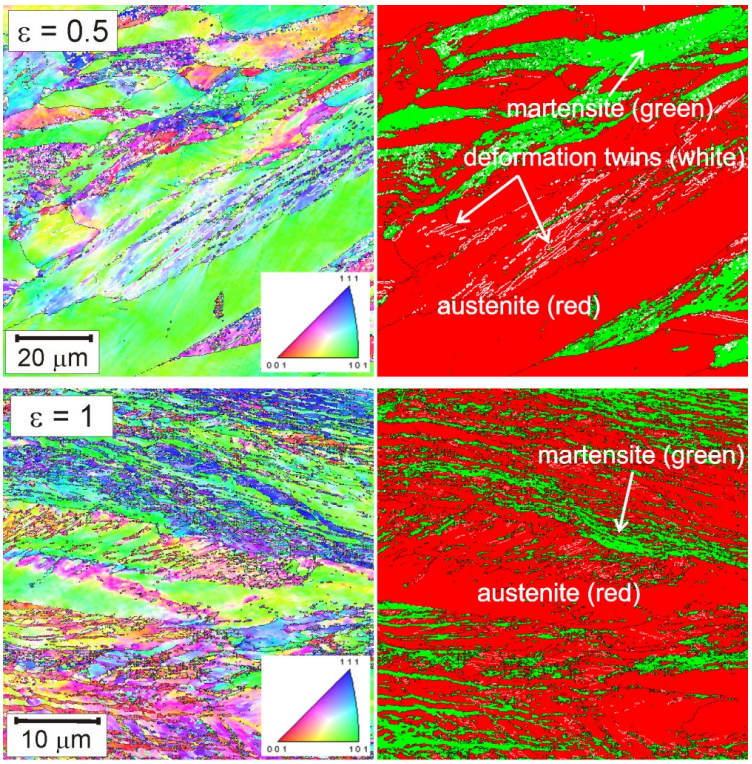

Figure 2. *Cont.*

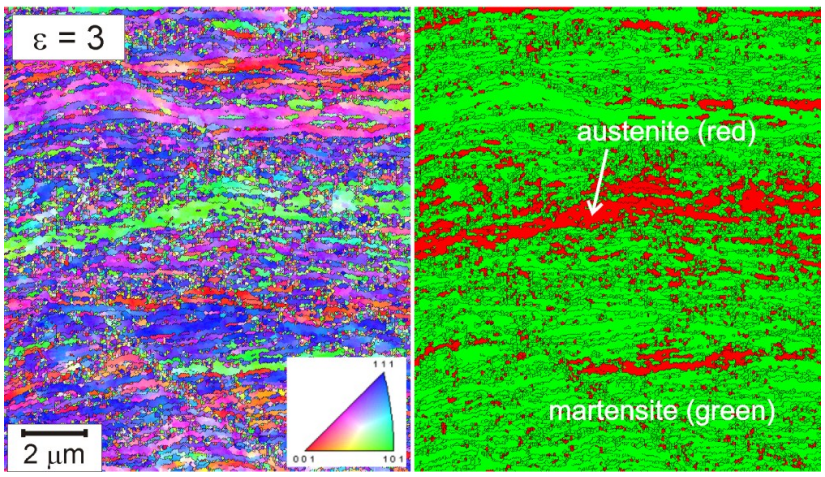

Figure 2. Deformation microstructures evolved in a 304L stainless steel during cold rolling various strains (ε). The black and white lines indicate the high-angle boundaries and twin boundaries, respectively. The inverse pole figures are shown for the normal direction.

Some details of the development of nanocrystalline structure in the present steel during cold rolling are shown in Figure 3. The microshear bands play an important role in the evolution of nanocrystalline structure. At intermediate strains, the strain-induced martensite readily develops at microshear bands. Hence, the microshear bands consist of alternating nanocrystallites of austenite and martensite (s. enlarged portion at ε = 1 in Figure 3). At large strains, the microshear bands cross over the flattened martensite crystallites. It should be noted that the martensite nanocrystallites evolved at large total strains are subdivided by high-angle grain boundaries (s. enlarged portion at ε = 3 in Figure 3).

The mechanisms of microstructure evolution during cold rolling are clearly reflected on the grain/phase boundary misorientation distributions evolved at different strain levels (Figure 4). The grain boundary misorientation distribution evolved at low to moderate stains of around 1 is characterized by three distinctive peaks against small angles below 10°, large angles around 45°, and large angles about 60°. The first of them is clearly associated with a number of low-angle deformation subboundaries that are commonly brought out by plastic deformation [2]. The second one around 45° results from martensitic transformation. The orientation relationships between austenite and martensite in stainless steels are close to those predicted by Kurdjumov-Sachs and Nishiyama-Wasserman, which result in misorientations of 42.9° and 46°, respectively, between austenite and martensite [9]. The third peak against 60° is, evidently, produced by deformation twinning, because the twin boundary misorientation in austenite is 60° around <111>. The misorientations of deformation subboundaries progressively increase during deformation [2]. Therefore, the fraction of low-angle subboundaries gradually decreases with increase in total strain. The pronounced deformation twinning at low to moderate strains seems to be exhausted at large strains. The corresponding 60° peak disappears at large strains. On the other hand, the strain-induced martensite continuously develops during the present cold rolling to a total strain of 3. It should be noted that grain boundaries in largely strained metals and alloys tend to exhibit random misorientation [2,24–26]. Therefore, the boundary misorientation distribution evolved in the stainless steel at large rolling strains looks like random distribution, which is superimposed with two peaks against small angles (deformation subboundaries are continuously developed) and large angles of 45° (resulting from martensitic orientation relationship).

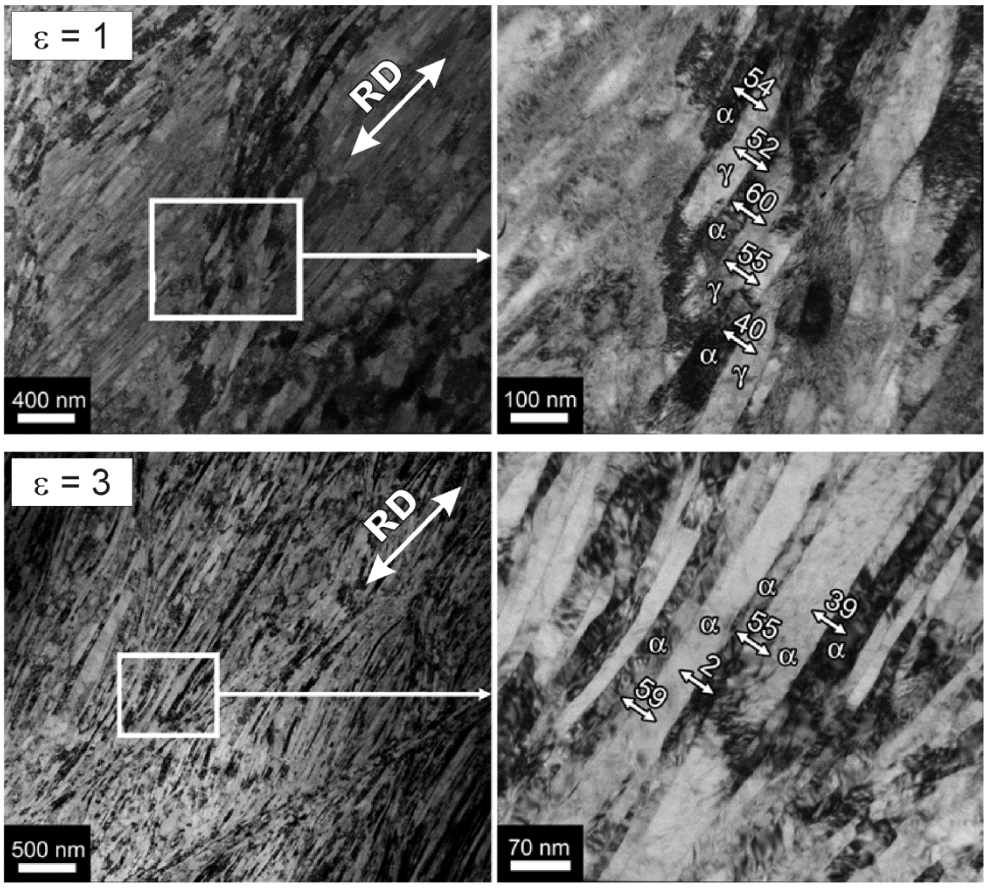

Figure 3. Fine structures evolved in a 304L stainless steel subjected to cold rolling to total strains of ε =1 and ε = 3. The RD indicates the rolling direction. The numbers indicate the boundary misorientations in degrees.

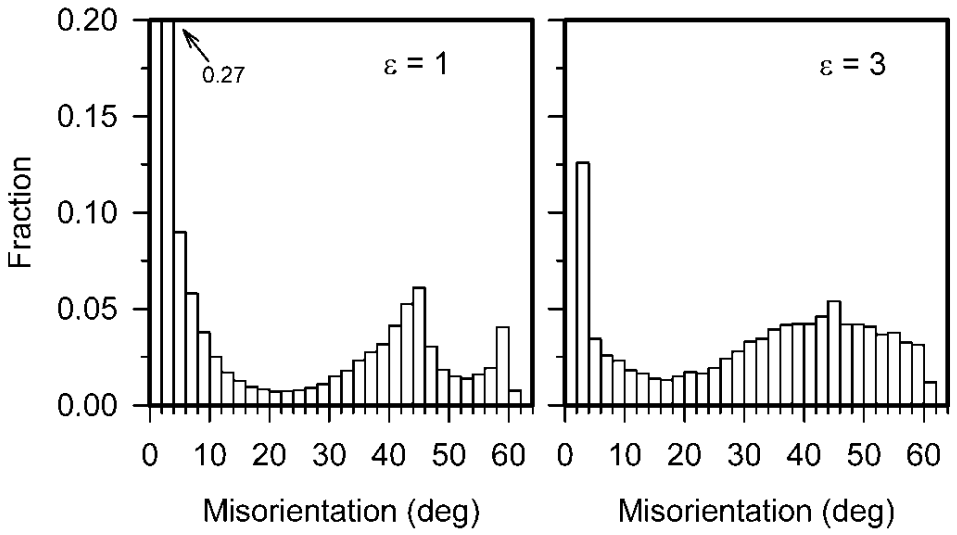

Figure 4. Grain boundary misorientation distributions evolved in a 304L stainless steel subjected to cold rolling to total strains of ε =1 and ε = 3.

The strain effect on the transverse grain size and the dislocation density during cold rolling of the stainless steel (Figure 5) correlates with the strain hardening (Figure 1). The austenite grain size rapidly reduces to about 700 nm upon cold rolling to a strain of 1. Then, the strain effect on the grain

refinement becomes less pronounced as strain increases. The transverse grain size of austenite gradually decreases to about 150 nm during cold rolling to a strain of 3. The transverse grain size of strain-induced martensite is characterized by similar strain dependence, although the martensite grains are finer than the austenite ones, especially, at relatively small strains. The martensite grain size finally attains about 120 nm at a total strain of 3. The dislocation density rapidly increases above 10^{15} m^{-2} at early deformation. Further cold rolling is accompanied by gradual increase in the dislocation density, which finally attains about 3×10^{15} m^{-2} in austenite and 2×10^{15} m^{-2} in martensite. A relatively low dislocation density in martensite may result from enhanced recovery in *bcc*-lattice.

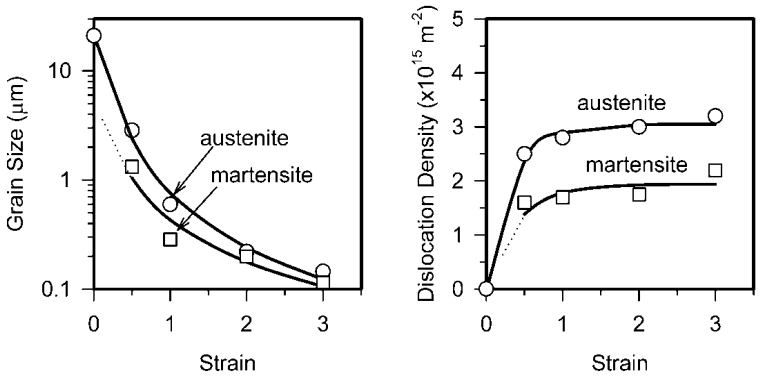

Figure 5. The effect of cold rolling strain on the transverse grain size and dislocation density in austenite and strain-induced martensite in a 304L stainless steel.

3.3. Tensile Behavior

The tensile stress-elongation curves for the 304L stainless steel subjected to cold rolling to different total strains are shown in Figure 6. The tensile behavior is characterized by a peak stress at relatively small strain followed by a decrease of the flow stress until fracture. The tensile strength increases, while the total elongation decreases with an increase in the previous rolling strain. The rolling to a strain of 3 results in significant increase in the yield strength from 220 MPa in the initial annealed state to 1600 MPa. The total elongation decreases correspondingly from 100% to 4%. Some microstructural parameters and mechanical properties of the steel samples cold rolled to different strains are listed in Table 1.

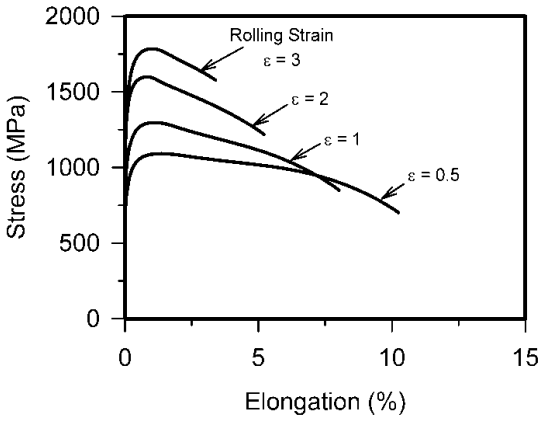

Figure 6. Engineering stress *vs.* plastic elongation curves for a 304L stainless steel subjected to cold rolling.

Table 1. The strain-induced martensite fraction (F_M), the grain size (D), the dislocation density (ρ), the yield strength ($\sigma_{0.2}$), the ultimate tensile strength (UTS), and the total elongation (δ) of a 304L stainless steel subjected to cold rolling to different strains (ε). The indexes of A and M indicate the austenite and martensite, respectively.

ε	F_M	D_A, μm	D_M, μm	ρ_A, 10^{14} m^{-2}	ρ_M, 10^{14} m^{-2}	$\sigma_{0.2}$, MPa	UTS, MPa	δ, %
0	0	21	-	0.02	-	220	600	100
0.5	0.20	2.85	1.33	25	16	950	1090	10
1	0.35	0.6	0.29	28	17	1160	1295	8
2	0.65	0.22	0.2	30	18	1485	1600	5
3	0.75	0.145	0.115	32	22	1595	1785	4

3.4. Strengthening Mechanisms

The yield strength of the present 304L steel subjected to large strain cold rolling can be expressed by the modified Hall-Petch relationship (Equation (1)), taking into account separate contributions of austenite and martensite to overall strength:

$$\sigma_{0.2} = F_A(\sigma_{0A} + K_{\varepsilon A}D_A^{-0.5} + \alpha_A G_A b_A \rho_A^{0.5}) + F_M(\sigma_{0M} + K_{\varepsilon M}D_M^{-0.5} + \alpha_M G_M b_M \rho_M^{0.5}) \quad (2)$$

where indexes of A and M indicate austenite and martensite, respectively, F_A and F_M are the austenite and martensite fractions, *i.e.*, $F_A + F_M = 1$. The values of σ_0 and K_ε can be obtained from conventional Hall-Petch relationship. To clarify the Hall-Petch relationship for the present steel, several annealed samples with statically recrystallized microstructures were subjected to tensile tests. The corresponding relationship between the austenite grain size and the yield strength is shown in Figure 7. Note here that the grain sizes were evaluated as the mean grain boundary spacing, counting all high-angle boundaries including twin boundaries. It is clearly seen in Figure 7 that the yield strength can be related to the austenite grain size as follows:

$$\sigma_{0.2A} = 180 + 240D_A^{-0.5} \quad (3)$$

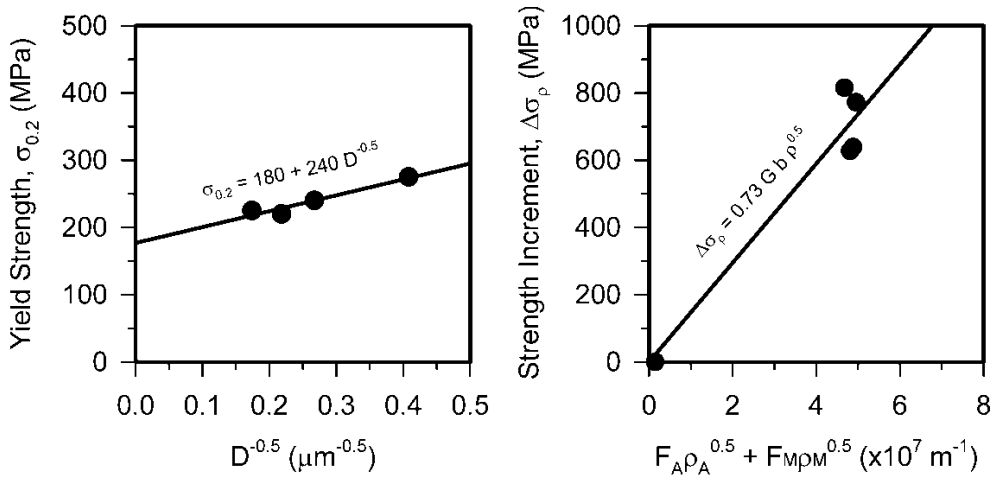

Figure 7. Hall-Petch relationship for a 304L stainless steel with annealed recrystallized microstructure and the effect of dislocation density (ρ) on the strength increment ($\Delta\sigma_\rho$).

The σ_{0A} = 180 MPa is quite close to those about 200 MPa reported for various austenitic steels [9,19,27]. The grain size strengthening in martensite can be evaluated by the following relationship, which has been obtained for recrystallized Fe–15%Cr steel [28]:

$$\sigma_{0.2M} = 180 + 240D_M^{-0.5} \quad (4)$$

Then, the dislocation strengthening can be estimated using the obtained data. The strength increment associated with dislocation strengthening from Equation (2) reads:

$$\Delta\sigma_\rho = \sigma_{0.2} - F_A\sigma_{0.2A} - F_M\sigma_{0.2M} = F_A\alpha_A G_A b_A \rho_A^{0.5} + F_M\alpha_M G_M b_M \rho_M^{0.5} \quad (5)$$

Note here that the shear modulus, G = 81 GPa, and Burgers vector, b = 0.25 nm, are almost the same for austenite and martensite (ferrite) [29]. Assuming that $\alpha_A = \alpha_M$, Equation (5) can be simplified as follows:

$$\Delta\sigma_\rho = \alpha Gb\,(F_A\rho_A^{0.5} + F_M\rho_M^{0.5}) \quad (6)$$

Figure 7 shows the relationship between the dislocation density and the corresponding strength increment. Thus, the value of α = 0.73 is obtained from Figure 7. It should be noted that almost the same values of α have been used for calculation of dislocation strengthening in various alloys [19–21,30–32]. Finally, the following expression for the yield strength of the present steel subjected to cold rolling can be obtained:

$$\sigma_{0.2} = F_A 180 + F_M 120 + 240(F_A D_A^{-0.5} + F_M D_M^{-0.5}) + 0.73Gb(F_A\rho_A^{0.5} + F_M\rho_M^{0.5}) \quad (7)$$

The relationship between the experimental yield stress and calculated by Equation (7) is shown in Figure 8. It is clearly seen that the yield strengths obtained by the modified Hall-Petch type equation are quite coincident with the experimental results. Figure 8 also shows the contributions of different strengthening mechanisms, *i.e.*, the austenite dislocation density ($\Delta\sigma_{\rho A}$), the austenite grain size ($\Delta\sigma_{DA}$), the martensite dislocation density ($\Delta\sigma_{\rho M}$), and the martensite grain size ($\Delta\sigma_{DA}$), into overall strength, taking into account the change in the austenite/martensite fraction during cold rolling. At small to moderate strains, the strengthening of the cold worked austenitic stainless steel is mainly provided by drastic increase in the dislocation density in the austenite. The strength contribution from austenite grain size becomes comparable with that from austenite dislocation density at rather large strains, when the grain size decreases to nano-scale level. The dislocation density and grain size of strain-induced martensite contribute to overall strength in similar manner as the austenite does. Namely, the strength increment from dislocation density significantly exceeds that from grain size at relatively small strains, whereas the strength increments from dislocation density and grain size become almost the same at large strains. However, the difference between the strength increments from dislocation density and grain size in the strain-induced martensite is much less pronounced than that in the austenite in the range of moderate to large strains. After rolling to a large total strain of 3, the same strengthening from martensite dislocation density and martensite grain size is observed (Figure 8).

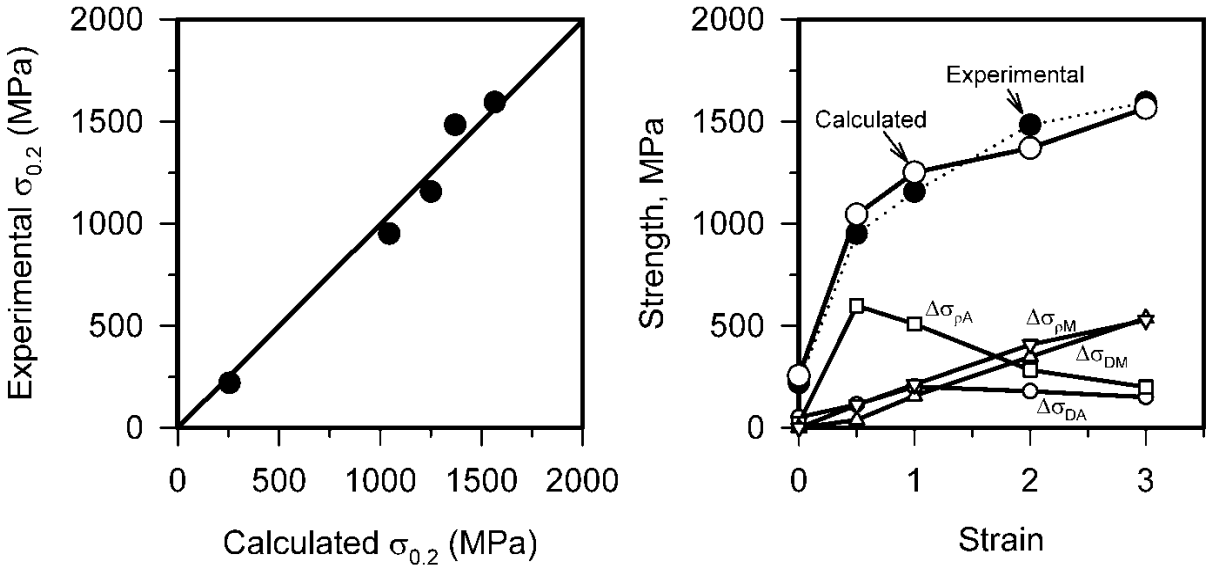

Figure 8. The relationship between experimental and calculated yield strength ($\sigma_{0.2}$) and the contribution of grain size strengthening ($\Delta\sigma_D$) and dislocation strengthening ($\Delta\sigma_\rho$) into overall strength on a 304L stainless steel subjected to cold rolling. The indexes of A and M indicate the austenite and martensite, respectively.

4. Conclusions

The microstructural evolution and corresponding mechanical properties of a 304L austenitic stainless steel subjected to large strain cold rolling at room temperature were studied. The main results can be summarized as follows:

1. The cold rolling was accompanied by a rapid increase in the dislocation density, which exceed 10^{15} m^{-2} after straining to 0.5. Features of microstructural changes in the austenitic stainless steel during cold deformation were the deformation twinning and the development of strain-induced martensitic transformation, which resulted in martensite fraction of 0.75 after rolling to a strain of 3. Both the deformation twinning and strain-induced martensite led to the rapid grain refinement. The nanocrystalline structure consisting of austenite and martensite grains with transverse grain sizes of 145 nm and 115 nm, respectively, was developed at a large total strain of 3.

2. The development of nanocrystalline structure provided significant strengthening. The yield strength increased from about 950 MPa to 1600 MPa with an increase in the total strain from 0.5 to 3. Considering the dislocation density (ρ) and grain size (D) as main contributors to overall strengthening, the following relationship for yield strength was obtained:

$$\sigma_{0.2} = F_A 180 + F_M 120 + 240(F_A D_A^{-0.5} + F_M D_M^{-0.5}) + 0.73Gb(F_A \rho_A^{0.5} + F_M \rho_M^{0.5})$$

where F_A and F_M are volume fractions of austenite and martensite, respectively, G is the shear modulus, b is Burgers vector, the indexes of A and M indicate austenite and martensite, respectively. The obtained results suggested that the strength increment from dislocation density remarkably exceeds that from grain size at small to moderate strains, whereas this difference gradually decreases during subsequent deformation to large total strains.

Acknowledgments

The authors gratefully acknowledge the financial support from the Ministry of Education and Science, Russia, (Belgorod State University project No. 1683). The authors are grateful to the personnel of the Joint Research Centre, Belgorod State University, for their assistance with the instrumental analysis.

Author Contributions

The present paper is a result of fruitful collaboration of all co-authors. R. Kaibyshev designed the research theme; A. Belyakov selected the experimental procedure; M. Odnobokova carried out the experimental study. Then, all co-authors discussed and analyzed the obtained results.

Conflicts of Interest

The authors declare no conflict of interest.

References

1. Valiev, R.Z.; Islamgaliev, R.K.; Alexandrov, I.V. Bulk nanostructured materials from severe plastic deformation. *Prog. Mater. Sci*. **2000**, *45*, 103–189.
2. Sakai, T.; Belyakov, A.; Kaibyshev, R.; Miura, H.; Jonas, J.J. Dynamic and post-dynamic recrystallization under hot, cold and severe plastic deformation conditions. *Prog. Mater. Sci*. **2014**, *60*, 130–207.
3. Valiev, R.Z.; Alexandrov, I.V.; Zhu, Y.T.; Lowe, T.C. Paradox of strength and ductility in metals processed by severe plastic deformation. *J. Mater. Res*. **2002**, *17*, 5–8.
4. Kimura, Y.; Inoue, T.; Yin, F.; Tsuzaki, K. Inverse temperature dependence of toughness in an ultrafine grain-structure steel. *Science* **2008**, *320*, 1057–1060.
5. Estrin, Y.; Vinogradov, A. Extreme grain refinement by severe plastic deformation: A wealth of challenging science. *Acta Mater*. **2013**, *61*, 782–817.
6. Stolyarov, V.V.; Valiev, R.Z.; Zhu, Y.T. Enhanced low-temperature impact toughness of nanostructured Ti. *Appl. Phys. Lett*. **2006**, *88*, 041905.
7. Misra, R.D.K.; Zhang, Z.; Venkatasurya, P.K.C.; Somani, M.C.; Karjalainen, L.P. Martensite shear phase reversion-induced nanograined/ultrafine-grained Fe–16Cr–10Ni alloy: The effect of interstitial alloying elements and degree of austenite stability on phase reversion. *Mater. Sci. Eng. A* **2010**, *527*, 7779–7792.
8. Rezaee, A.; Kermanpur, A.; Najafizadeh, A.; Moallemi, M. Production of nano/ultrafine grained AISI 201L stainless steel through advanced thermo-mechanical treatment. *Mater. Sci. Eng. A* **2011**, *528*, 5025–5029.
9. Shakhova, I.; Dudko, V.; Belyakov, A.; Tsuzaki, K.; Kaibyshev, R. Effect of large strain cold rolling and subsequent annealing on microstructure and mechanical properties of an austenitic stainless steel. *Mater. Sci. Eng. A* **2012**, *545*, 176–186.

10. Belyakov, A.; Odnobokova, M.; Kipelova, A.; Tsuzaki, K.; Kaibyshev, R. Nanocrystalline structures and tensile properties of stainless steels processed by severe plastic deformation. *IOP Conf. Ser. Mater. Sci. Eng*. **2014**, *63*, 012156.
11. Olson, G.B.; Cohen, M. Kinetics of strain-induced martensitic nucleation. *Metall. Trans. A* **1975**, *6A*, 791–795.
12. Nakada, N.; Ito, H.; Matsuoka, Y.; Tsuchiyama, T.; Takaki, S. Deformation-induced martensitic transformation behavior in cold-rolled and cold-drawn type 316 stainless steels. *Acta Mater*. **2010**, *58*, 895–903.
13. Lee, T.-H.; Shin, E.; Oh, C.-S.; Ha, H.-Y.; Kim, S.-J. Correlation between stacking fault energy and deformation microstructure in high-interstitial-alloyed austenitic steels. *Acta Mater.* **2010**, *58*, 3173–3186.
14. Armstrong, R.; Codd, I.; Douthwaite, R.M.; Petch, N.J. The plastic deformation of polycrystalline aggregates. *Philos. Mag*. **1962**, *7*, 45–58.
15. Mecking, H.; Kocks, U.F. Kinetics of flow and strain-hardening. *Acta Metall*. **1981**, *29*, 1865–1875.
16. Estrin, Y.; Toth, L.S.; Molinari, A.; Brechet, Y. A dislocation-based model for all hardening stages in large strain deformation. *Acta Mater*. **1998**, *46*, 5509–5522.
17. Hughes, D.A.; Hansen, N. Microstructure and strength of nickel at large strains. *Acta Mater*. **2000**, *48*, 2985–3004.
18. Hansen, N. Hall-Petch relation and boundary strengthening. *Scr. Mater*. **2004**, *51*, 801–806.
19. Yanushkevich, Z.; Mogucheva, A.; Tikhonova, M.; Belyakov, A.; Kaibyshev, R. Structural strengthening of an austenitic stainless steel subjected to warm-to-hot working. *Mater. Charact*. **2011**, *62*, 432–437.
20. Kusakin, P.; Belyakov, A.; Haase, C.; Kaibyshev, R.; Molodov, D.A. Microstructure evolution and strengthening mechanisms of Fe–23Mn–0.3C–1.5Al TWIP steel during cold rolling. *Mater. Sci. Eng. A* **2014**, *617*, 52–60.
21. Mishnev, R.; Shakhova, I.; Belyakov, A.; Kaibyshev, R. Deformation microstructures, strengthening mechanisms, and electrical conductivity in a Cu–Cr–Zr alloy. *Mater. Sci. Eng. A* **2015**, *629*, 29–40.
22. Kipelova, A.; Odnobokova, M.; Belyakov, A.; Kaibyshev, R. Microstructure evolution in a 304-type austenitic stainless steel during multidirectional forging at ambient temperature. *Mater. Sci. Forum* **2014**, *783–786*, 831–836.
23. Odnobokova, M.; Kipelova, A.; Belyakov, A.; Kaibyshev, R. Microstructure evolution in a 316L stainless steel subjected to multidirectional forging and unidirectional bar rolling. *IOP Conf. Ser. Mater. Sci. Eng*. **2014**, *63*, 012060.
24. Mishin, O.V.; Gottstein, G. Microstructural aspects of rolling deformation in ultrafine-grained copper. *Philos. Mag. A* **1998**, *78*, 373–388.
25. Mishin, O.V.; Bowen, J.R.; Lathabai, S. Quantification of microstructure refinement in aluminium deformed by equal channel angular extrusion: Route A vs. route Bc in a 90° die. *Scr. Mater*. **2010**, *63*, 20–23.
26. Tikhonova, M.; Kuzminova, Y.; Fang, X.; Wang, W.; Kaibyshev, R.; Belyakov, A. Σ3 CSL boundary distributions in an austenitic stainless steel subjected to multidirectional forging followed by annealing. *Philos. Mag*. **2014**, *94*, 4181–4196.

27. Young, C.M.; Sherby, O.D. Subgrain formation and subgrain-boundary strengthening in iron-based materials. *J. Iron Steel Inst*. **1973**, *211*, 640–647.
28. Belyakov, A.; Tsuzaki, K.; Kimura, Y.; Mishima, Y. Tensile behaviour of submicrocrystalline ferritic steel processed by large-strain deformation. *Philos. Mag. Lett*. **2009**, *89*, 201–212.
29. Frost, H.J.; Ashby, M.F. *Deformation Mechanism Maps*; Pergamon Press: Oxford, UK, 1982.
30. Huang, X.; Morito, S.; Hansen, N.; Maki, T. Ultrafine structure and high strength in cold-rolled martensite. *Metall. Mater. Trans. A* **2012**, *43A*, 3517–3531.
31. Harrell, T.J.; Topping, T.D.; Wen, H.; Hu, T.; Schoenung, J.M.; Lavernia, E.J. Microstructure and strengthening mechanisms in an ultrafine grained Al-Mg-Scalloy produced by powder metallurgy. *Metall. Mater. Trans. A* **2014**, *45A*, 6329–6343.
32. Khamsuk, S.; Park, N.; Gao, S.; Terada, D.; Adachi, H.; Tsuji, N. Mechanical properties of bulk ultrafine grained aluminum fabricated by torsion deformation at various temperatures and strain rates. *Mater. Trans*. **2014**, *55*, 106–113.